Iridium Optical Constants for the Chandra X-Ray Observatory from Reflectance Measurements of 0.05-12 keV

D.E. Graessle[*a], R. Soufli[b], A.L. Aquila[c], E.M. Gullikson[c], R.L. Blake[d], A.J. Burek[e]
[a]Smithsonian Astrophysical Observatory, MS-70, Cambridge, MA 02138-5620;
[b]Lawrence Livermore National Laboratory, 7000 East Avenue, L-395, Livermore, CA 94550-9234;
[c]Lawrence Berkeley Laboratory, 1 Cyclotron Rd, MS-2R0400, Berkeley, CA 94720;
[d]RDS, PO Box 6880, Santa Fe, NM 87502-6880;
[e]SFA Inc, Largo, MD 20774

ABSTRACT

We present optical constants derived from synchrotron reflectance measurements of iridium-coated X-ray witness mirrors over 0.05-12 keV, relevant to the Chandra X-ray Observatory effective area calibration. In particular we present for the first time analysis of measurements taken at the Advanced Light Source Beamline 6.3.2 over 50-1000 eV, Chandra's lower-energy range. Refinements to the currently tabulated iridium optical constants (B. L. Henke et al., At. Data Nucl. Data Tables 54, 181-343, 1993 and on the Web at http://www-cxro.lbl.gov/optical_constants/) will become important as the low-energy calibration of Chandra's X-ray detectors and gratings are further improved, and as possible contaminants on the Chandra mirror assembly are considered in the refinement of the in-flight Ir absorption edge depths. The goal of this work has been to provide an improved tabulation of the Ir optical constants over the full range of Chandra using a self-consistent mirror model, including metallic layers, interface roughness, contaminating overlayer, and substrate. The low-energy data present us with a considerable challenge in the modeling of the overlayer composition, as the K-absorption features of C, O, and N are likely to be present in the ~10A overlayer. The haphazard contamination and chemical shifts may significantly affect optical constants attributed to this overlayer, which will distort the iridium optical constants derived. Furthermore, the witness mirror contamination may be considerably different from that deposited on the flight optics. The more complex modeling required to deal with low-energy effects must reduce to the simpler model applied at the higher energies, which has successfully derived optical constants for iridium in the higher energy range, including the iridium M-edges, already used in the Chandra calibration. We present our current results, and the state of our modeling and analysis, and our approach to a self-consistent tabulation.

KEYWORDS: Chandra X-ray Observatory, iridium, optical constants, reflectance, X-ray mirrors, grazing incidence

1. INTRODUCTION

Included in the coating process for the eight mirror elements of Chandra's High Resolution Mirror Assembly (HRMA) were numerous witness mirrors. More than fifty of these mirrors were designated for reflectance calibrations at various synchrotron laboratories, so that optical constants for the coatings could be derived for the full 50-12000 eV range, including all spectral features (absorption edges). A schematic showing the positions of the various witness mirrors during qualification (no HRMA element present) and production (HRMA element and off-end witness mirrors) coating runs is shown in Figure 1. A few of these mirrors were 2" circular disks, with super-polished surfaces giving less than one angstrom of micro-roughness over the 0.5-500 micron spatial scales. These mirrors, polished by General Optical Co. of Moorpark, CA, were used in position "A1" in the figure, and hence were present in all sixteen coating runs. For the present paper we shall confine our discussions to those mirrors only.

*dgraessle@head-cfa.harvard.edu; phone 1 617 495-7041; fax 1 617 495-7356; head-cfa.harvard.edu/~graessle.
Copyright 2004 Society of Photo-Optical Instrumentation Engineers. This paper was published in *X-ray and Gamma-Ray Instrumentation for Astronomy XIII*, Kathryn A Flanagan and Oswald H.W. Siegmund, editors, Proceedings of SPIE vol. **5165**, p. 469, 2004, and is made available as an electronic reprint with permission of SPIE. One print or electronic copy may be made for personal use only. Systematic or multiple reproduction, distribution to multiple locations by electronic or other means, duplication of any material in this paper for a fee or for commercial purposes, or modification of the content of the paper are prohibited.

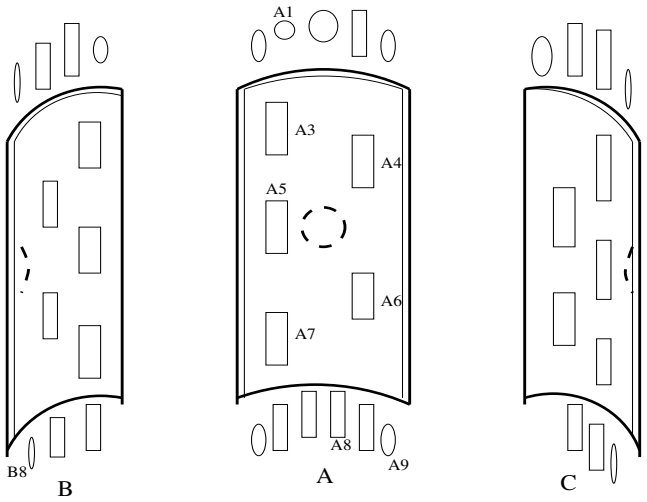

NOTE THREE LONGITUDINAL SECTIONS:A, B and C

OUTBOARD SAMPLES BECAME PRODUCTION WITNESS FLATS

Figure 1: Schematic of the witness coupon configuration used in the Chandra coating process. The position marked "A1" is the location in the coating process of the super-smooth mirrors discussed in this paper.

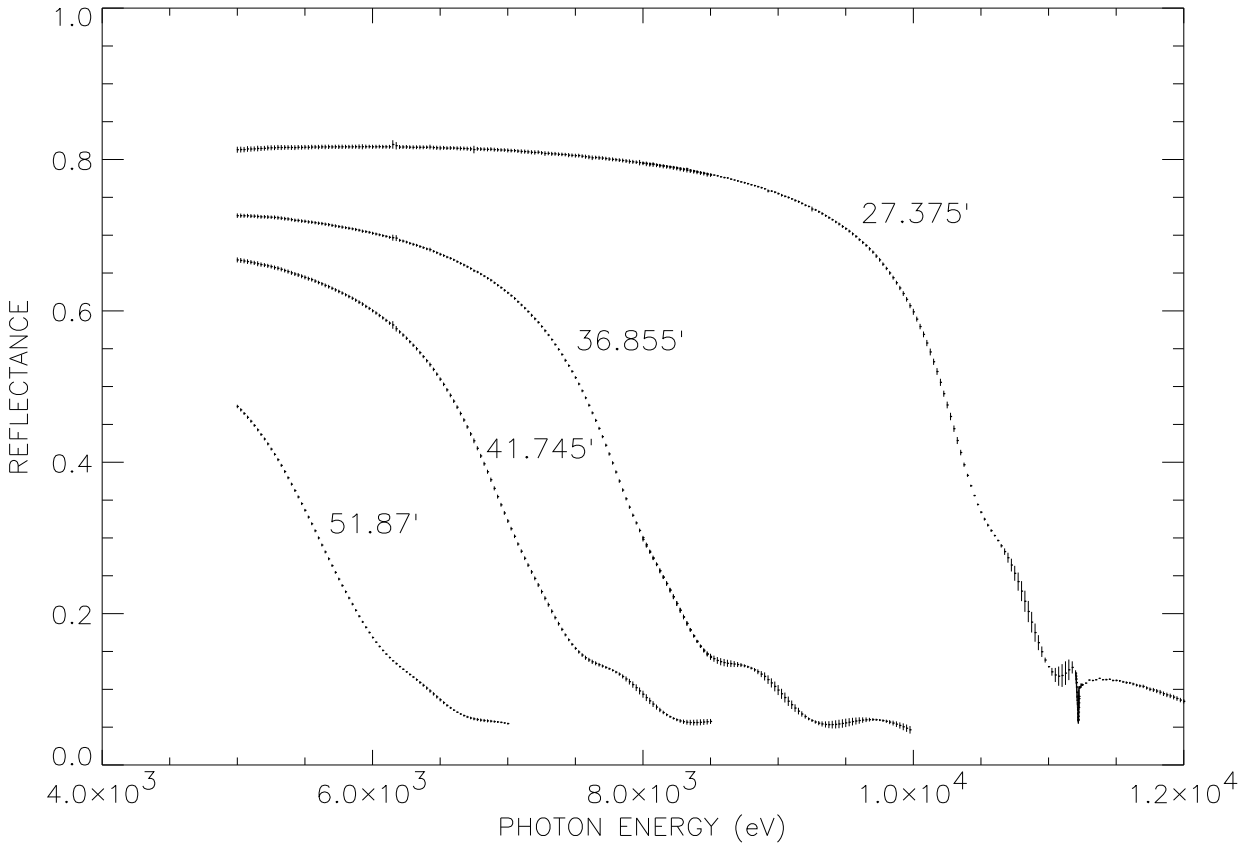

Figure 2: Average reflectance values with standard deviations (vertical error bars) at the four Chandra principle grazing angles, over 5-12 keV. Sixteen super-smooth mirrors are included in the average. Excluding the interference fringes, the standard deviations are within 0.5%.

When last we presented out results to SPIE in 1998[1], we reported extremely consistent measurements for the sixteen coating runs for Chandra mirror elements, provided that only the super-smooth mirrors were considered. Figure 2 shows the individual reflectance points in the 5-12 keV range, plotted as vertical error bars representing the standard deviations of the averages of sixteen mirror reflectances from sixteen different coating runs. The four grazing angles presented are the principle grazing angles for the four mirror shells of Chandra. The mirrors are within less than one-half percent relative variation until the layer depths are considered, which results in the larger mirror-to-mirror variations at the interference fringes below 10% reflectance.

We have used the NKFIT analysis package developed by D.L. Windt, a package which has since been greatly enhanced and is now available as part of the IMD package[2]. The model used in our 1998 analysis of 5-12 keV data was a three-layer model (excluding the incident vacuum medium) as illustrated in Fig. 3. The energy loss due to roughness had been found by testing to be in agreement with the model of Nevot and Croce[3], where a perfect vertical correlation of the roughness between each layer is assumed. The result of this assumption in the derivation is that there is essentially no scattering loss in the model below the critical grazing angle, and a steeper energy loss beyond the critical angle than would be predicted from the model of Stearns et al.[4]

A fit of a 10 keV angle scan (Fig. 4) for standard mirror 065 (the "A1" position mirror from the first qualification coating run for Chandra) gives significant residuals, particularly in the interference fringes at large grazing angles. Hence, we used a two-step fitting method to derive the best optical constants, in the absence of an explanation for the residuals. The first fit was used to identify the underlayer parameters such as coating thickness and interface roughness. Fixing those values, we then ran a second fit of the data down to reflectance values of 1%. The second fit would indicate how well one would expect to fit energy scan data, wherein only a few (six to eight) angle data points would be included for each energy, and those measured values would be fitted, holding all other parameters fixed, for only the optical constants n and k of the iridium coating layer.

We show the fitted results for optical constants δ, the refractive decrement (=1-n) and β, the extinction coefficient (=k) in Fig. 5, for the 5-12 keV range. The tabulated optical constants from Henke et al, 1993[5], are shown for comparison. For the super-smooth GO mirrors, both δ(E) and β(E) are extremely consistent. However, β(E) shows about twice the scatter in the data, indicating that it is the more sensitive of the two to reflectivity variations between mirrors.

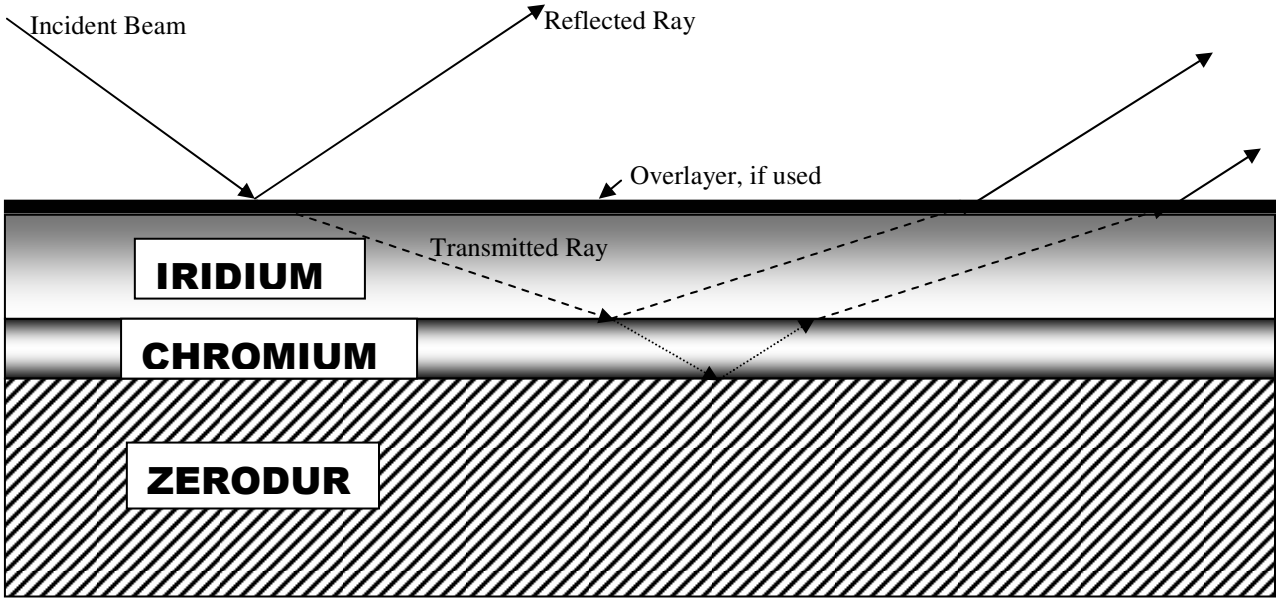

Figure 3: Multiple layer model used in NKFIT to characterize the mirrors in this paper. The overlayer is introduced in Section 2.

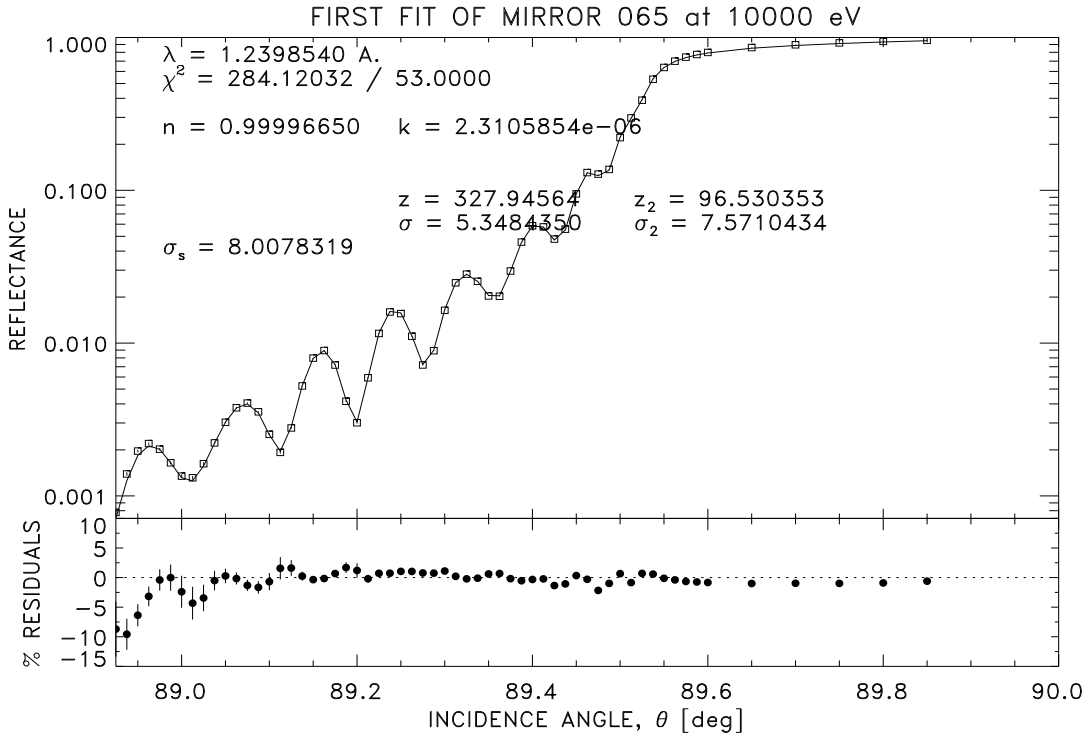

Figure 4: Seven-parameter fit (top) of 10 keV angle scan of standard mirror 065, and the corresponding residuals of the fit (bottom). Here n and k are those if Ir, z is Ir depth, z_2 is Cr depth, σ is Ir surface roughness, σ_2 is Ir/Cr interface roughness, σ_3 is Cr/Zerodur roughness. Layer depths and roughness are in Angstroms.

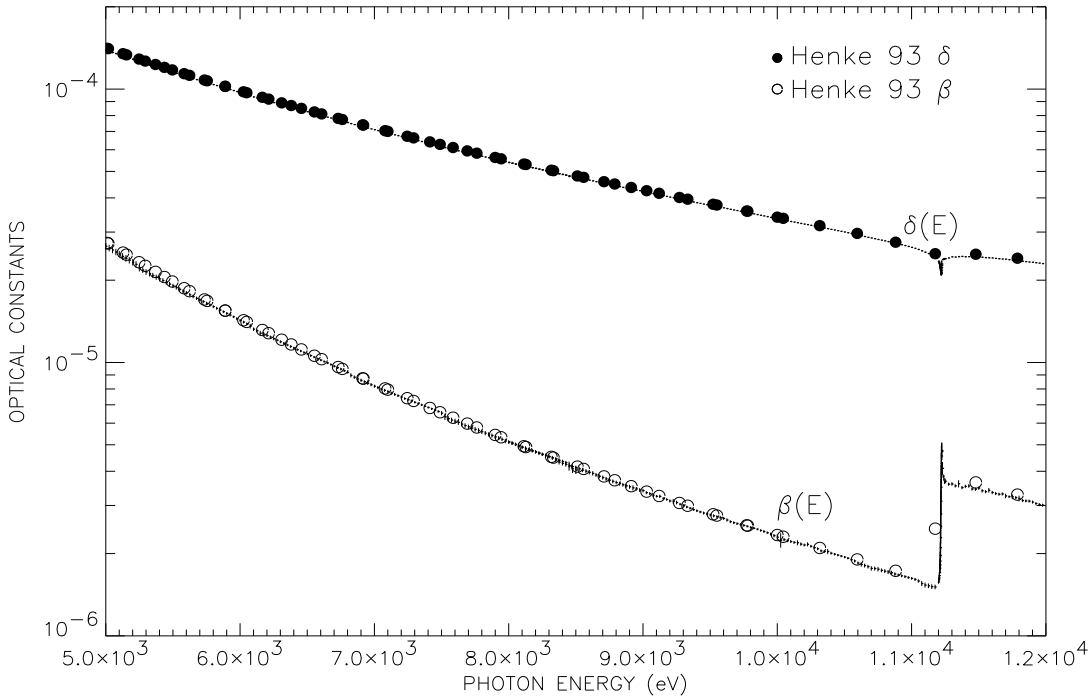

Figure 5: Optical constant $\delta(E)$ and $\beta(E)$ derived from Chandra the super-smooth GO witness mirrors. Each point is plotted as a vertical bar denoting the standard deviation of the average of sixteen mirrors.

2. MODELING THE M-EDGE RANGE 2010-2900 EV

The mirror reflectances in the M-edge region, by contrast, are not quite as consistent with one another as they are in the higher-energy ranges, even when only the super-smooth GO mirrors are considered. Fig. 6 gives the average values of measured reflectances from 16 mirrors, plotted as vertical error bars giving the standard deviation of the averages for those energy points, for the 2250-2900 eV range, which includes the M3 edge. The scatter in these measurements is greater by a factor of two than for the 5-10 keV range with the same mirrors. The distribution is not uniform, indicating an additional systematic effect must be considered in the analysis.

Considering, then, angle scans at 2550 eV with the three-layer model, the fitting results are as shown in Fig. 7, where a considerable systematic residual appears. This indicates another feature in the data requiring some enhancement in the model. We therefore added a uniform overlayer to the model, something which might be expected for these mirrors, though we currently only speculate regarding the chemical nature of that overlayer. For the present case, we have assumed a hydrocarbon chain of the form CH_2, with a density of $1 g/cm^3$. The optical constants were then derived from the tables of Ref. 5. The depth of the overlayer was treated as a free parameter in fitting angle scans, to determine whether a reasonable layer depth could be derived and applied to the fitting of energy scan data. An example of the improvement in the fits at 2550 eV is given in Fig. 8, where the same data are fit as in Fig. 7, but with the overlayer included in the model, and with the overlayer depth added as an additional free parameter. The results are quite striking. The residuals are at approximately the true noise level for this measurement. The fitted parameter values are as shown in the plot.

Having fitted for an overlayer at 2550 eV, it now remains to check the result at 10 keV with a similar overlayer model. Those results are shown in Fig. 9, with the same data as used previously in Fig. 4. The residuals here are considerably reduced as well, though not by an identical overlayer depth. Inasmuch as the same apparatus is used in each measurement, though a different beamline is employed, one might say that some nonuniformity of the overlayer is in evidence here, since a different range of angles being considered at 2550 eV than at 10 keV. It remains for us, as part of some future work, to quantify the overlayer independently in order to check the validity of these fitting results.

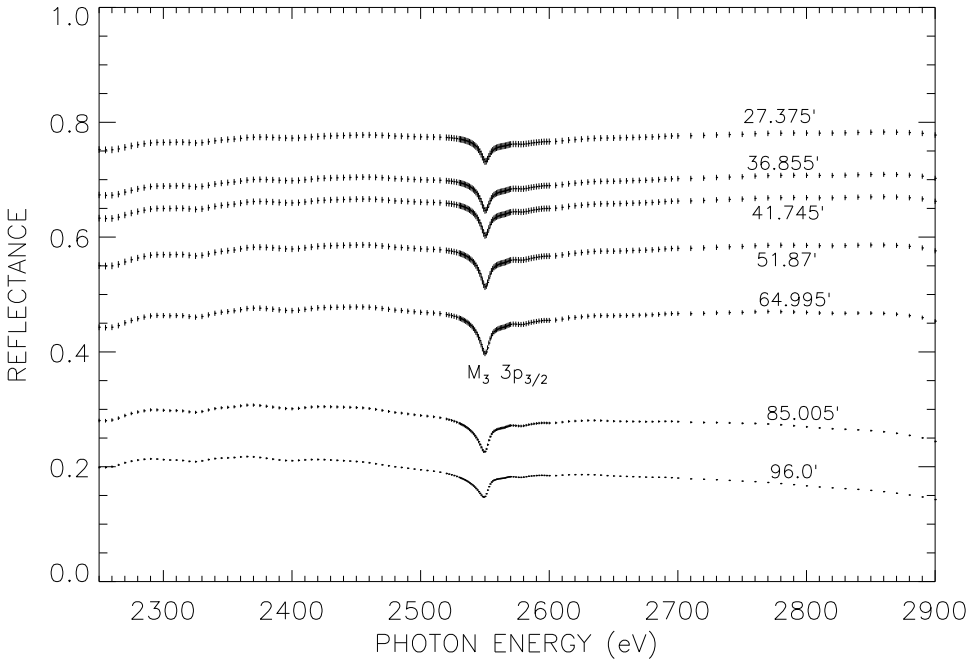

Figure 6: Reflectance versus energy for the M_3-edge range, averaged over eighteen GO mirrors. The standard deviation bars on these data are at a level of 0.8-1.2%, and the distribution is not uniform.

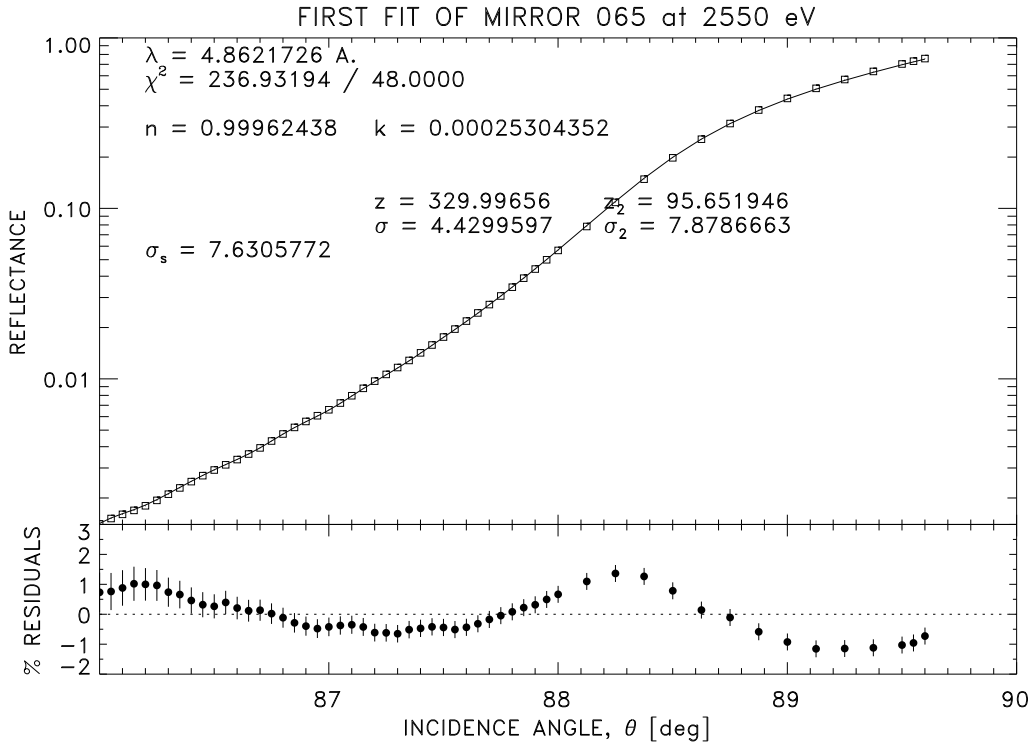

Figure 7: Three-layer, seven-parameter fit of standard mirror 065 at 2550 eV, with residuals. No overlayer is included.

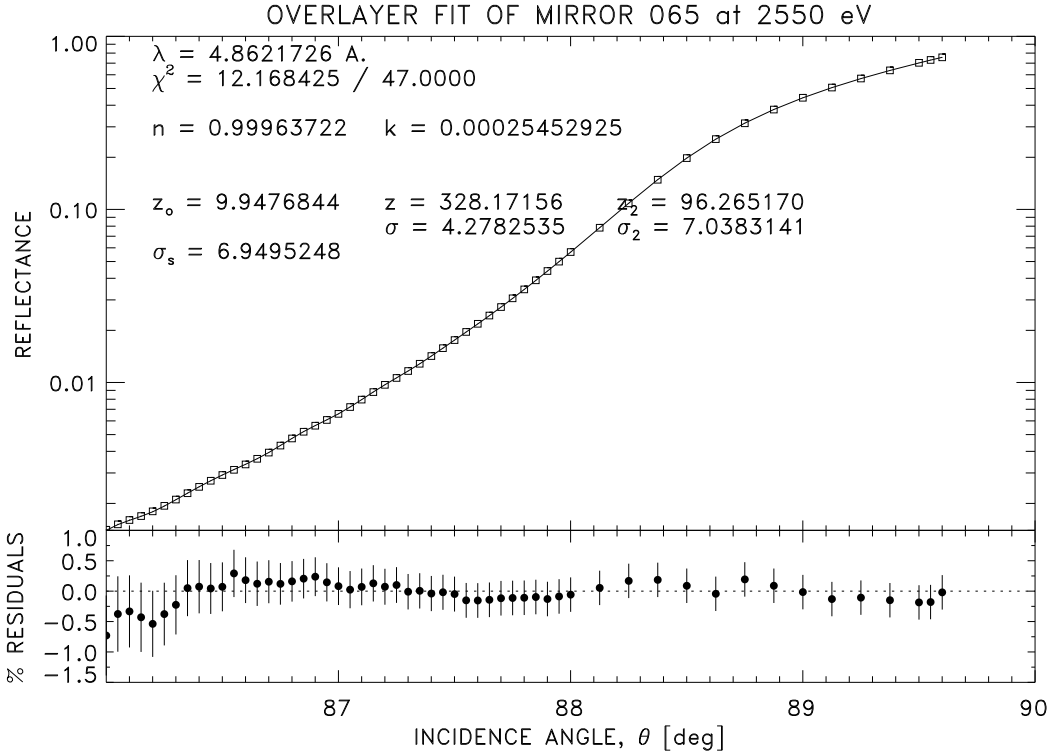

Figure 8: Fit of the same 2550 eV angle scan data as in Fig. 8, but this time with an overlayer included, and the depth of that layer as an eighth free parameter. Noise level in the data is approximately 0.2% relative. Here z_0 is the overlayer depth in Angstroms.

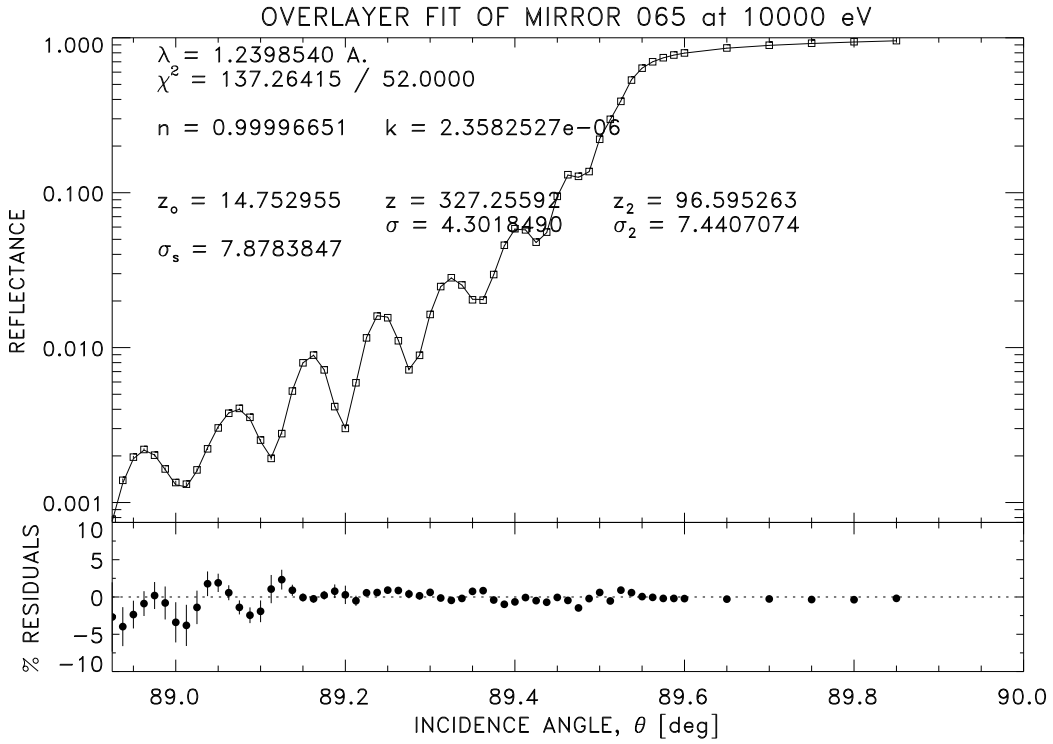

Figure 9: A fit of the same 10 keV data as in Fig. 4, but with an overlayer included, and the overlayer depth as an additional free parameter. Residuals are markedly improved over Fig. 4.

It should be pointed out that this overlayer is likely to be completely unrelated to any overlayer that may exist on Chandra's flight mirrors, as their storage and exposure histories are completely different. Notwithstanding, to the level of several angstroms, it seems that a basically consistent overlayer model might be developed for use over the full range of energies of the calibration, in order to characterize the optical constants of the iridium itself.

Completing this investigation of the M-edges, we give Fig. 10, the optical constants derived with and without including the overlayer in the model, for the M-edge region for the sixteen mirrors in question. When no overlayer is used, there is twice as much scatter in the derived $\beta(E)$ as there is when one is employed independently for each mirror. $\delta(E)$ is not affected, however. This lends credence to the notion that the effect is an overlayer masking effect, reducing the effective absorption by the iridium layer. The variation from mirror to mirror of the overlayer depth accounts essentially entirely for the enhanced relative error in the derived $\beta(E)$ when no overlayer is included. With the overlayer, the scatter in the results is 0.5% in δ and 2.5% in β, for these 16 mirrors. This is similar to the variations seen over the 5-12 keV range, in both optical constants.

Adding the 2010-6000 eV data to the optical constants derived for our standard mirror 065, we now have Fig. 11. Again the tabulated optical constants (Ref. 5) are provided for comparison. We note that there is now a disparity between the Henke and the 065 optical constants near 2.0 keV. Hence we had a need to extend measurements below 2010 eV, which was in fact accomplished using NSLS Beamline U3A.

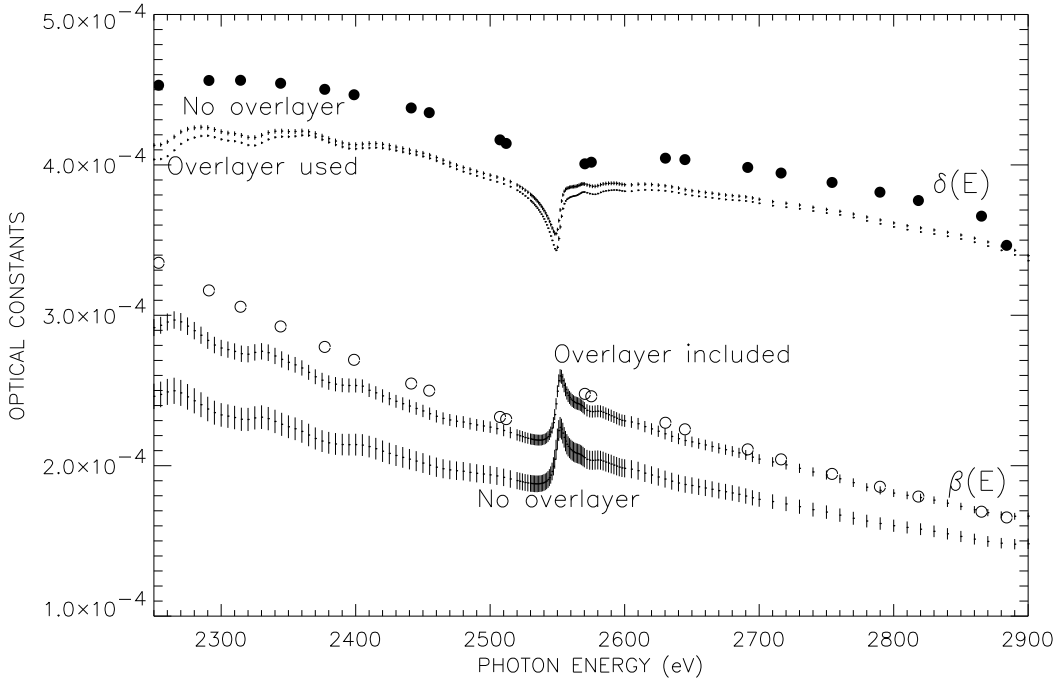

Figure 10: Optical constants derived in the M_3-edge range with and without an overlayer included in the model. Henke 1993 constants are included as solid or open dots. The derived data are plotted as vertical error bars denoting the standard deviation of the average for each point in the energy scans.

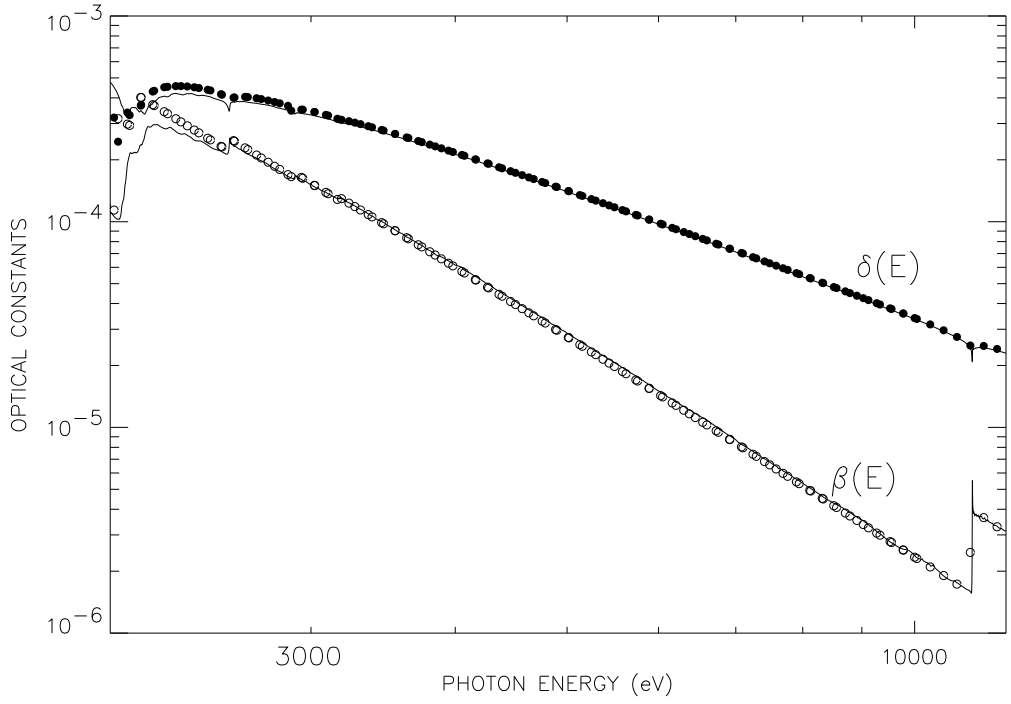

Figure 11: Chandra calibrated optical constants over 2-12 keV (curves). Ref. 5 tabulated optical constants are plotted as symbols.

3. THE CHANDRA COATING CALIBRATION 0.940-12.0 KEV

Only a few of the 2" mirrors were calibrated on Beamline U3A[6], due to the broad beam width, which is not conducive to small angle measurements on smaller mirrors. Hence we will not be presenting averages of sixteen GO mirrors in this section. However, the standard mirror 065 was indeed measured on U3A, and the results of all reflectance versus energy scans taken on that mirror are shown in Fig. 12, with angles in arc minutes identified. The energy range was divided up into two separate scanning ranges for optimal beamline monochromator performance, namely 940-1300 eV and 1280-2030 eV. Note that in Fig. 12 we include some 2010-2100 eV data points taken on Beamline X8A. There is good overlap between reflectance data taken on the two different beamlines.

Angle scans at 1200 eV and 1800 eV were taken of this flat as well, as a means of determining the alignment quality for each energy subrange. In analysis of the energy scan data, we used the fitting results from 2550 eV rather than those from 1200 eV or 1800 eV, with the optical constants determined as given in Fig. 13 for the U3A range. The residuals for these fits are extremely low, and the overlap with the X8A results at 2010-2030 eV is quite good, generally within 1%, and so the extension of the energy range to U3A was quite successful. By measuring these optical constants, we were able to eliminate the artificial jump that would have been created by joining X8A results above 2010 eV with tabulated values below that energy.

With the inclusion of the optical constants derived from Beamline U3A, and the inclusion of Henke 1993 optical constants for the lower energy range (50-940 eV), we obtain the current calibration standard for the Chandra HRMA iridium optical constants, presented in Fig. 14. The overlap error between the Henke data and our derived data at 940-1000 eV is relatively small. Refinement of the 50-1000 eV optical constants requires the analysis of data taken from Beamline 6.3.2 of the Advanced Light Source, discussed in the next section. These data have already been used in an earlier presentation of the HRMA effective area.[7]

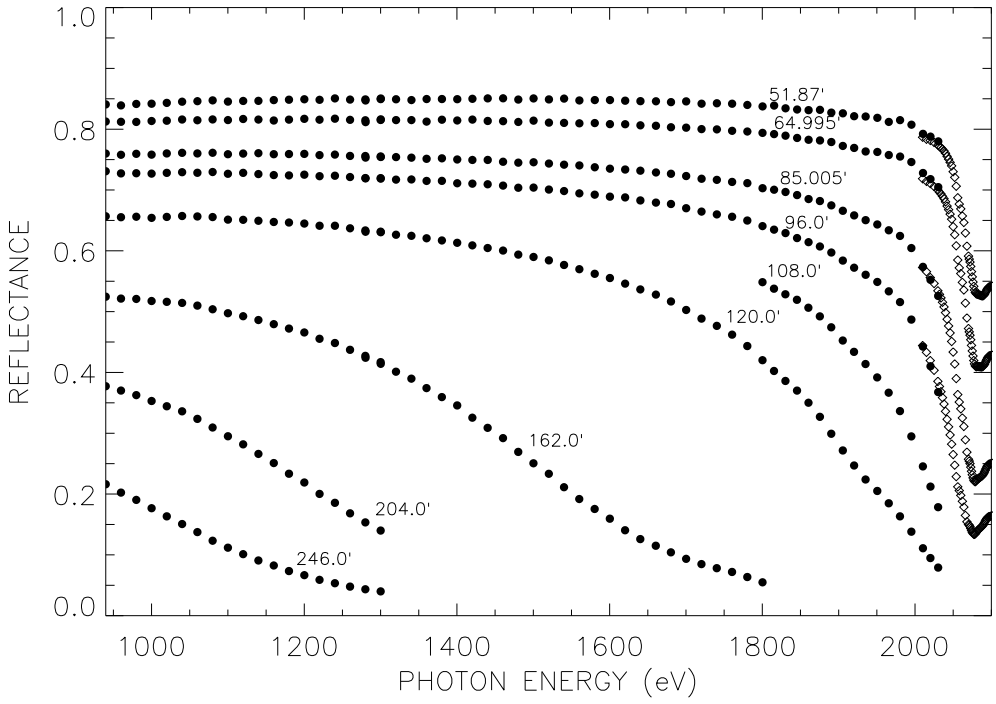

Figure 12: Reflectance versus energy scans for standard mirror 065 in the 940-2030 eV range. The open diamonds on the right side correspond to measurements on the X8A beamline which begin at 2010 eV.

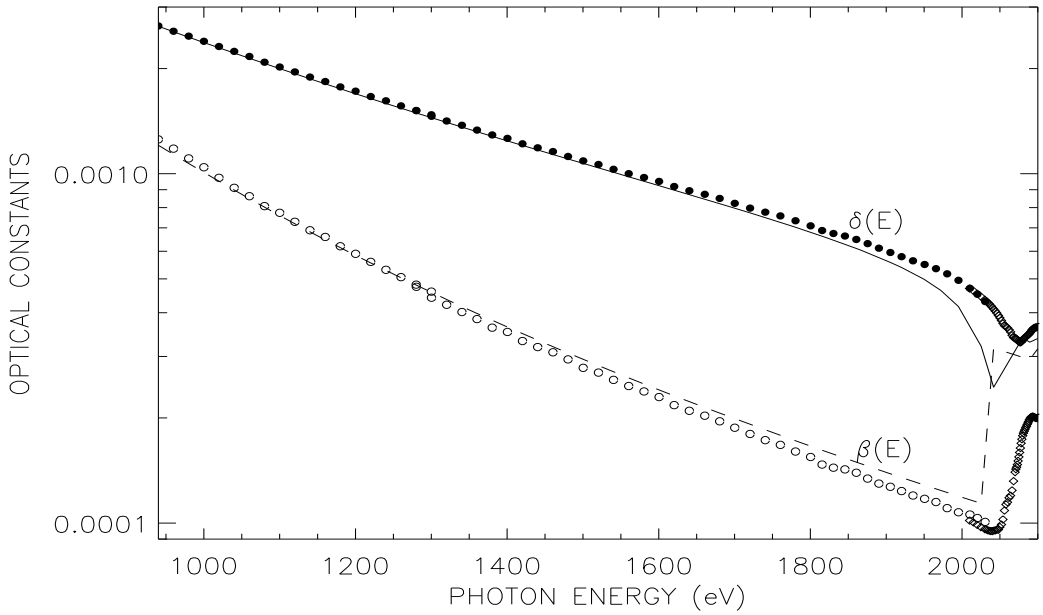

Figure 13: Optical constants derived for the 940-2030 eV range, for standard mirror 065, derived from Beamline U3A data. Diamond symbols at the right represent values derived from X8A data. Tabulated values (ref. 5) are plotted as curves for comparison.

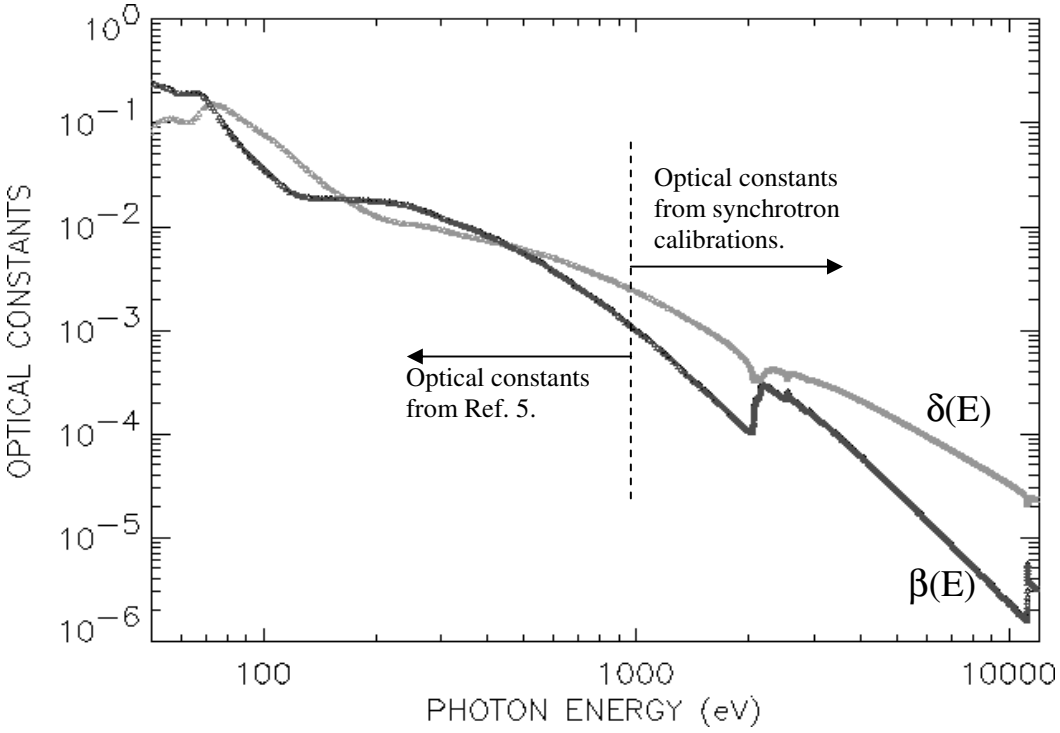

Figure 14: The current calibration standard for Chandra iridium optical constants. These data are directly from Henke 1993 for the 50-940 eV energy range. For the 940-12000 eV range, these data are the optical constants derived from standard mirror 065. They are not averaged over many mirrors at this stage.

4. ALS MEASUREMENTS: 50-1300 EV

Some of the most difficult measurements and modeling to be done for the calibration of Chandra witness mirrors occurs at the lowest energy range for the mission, specifically below 1000 eV. The challenges in this energy region are (1) to gain access to a high-stability, high spectral purity low-energy beamline with reflectometer access, and (2) the quantification of low-Z contaminants in any overlayer(s) that might be present on the mirrors. ALS Beamline 6.3.2[8] gives more than an adequate solution to issue 1. The second issue involves considerably more work.

Above 1000 eV, representation of a thin overlayer using a simple hydrocarbon chain is fine, as long as none of the elements actually present in the overlayer have absorption features in the energy range of interest. However, this will not work at all below 1000 eV, where those low-Z absorption edges are abundant. Here the characterization of any contaminating layer must be detailed and exact, including elemental composition and chemical shifts. Simple admixtures of C, N, and O will not suffice for a continuous determination of optical constants for iridium over the entire energy band. This is a work in progress, and we report only preliminary results from our standard mirror 065 at this point.

In order to assure the highest beam purity and intensity possible over the full 50-1300 eV band, this range must be broken down into numerous subintervals, wherein for each case optimal beam filtration and higher order suppression are set, and alignments of mirror sample to beam must be done independently. A total of twelve subintervals were selected to optimize beam purity and alignment accuracy for the Chandra reflectance calibrations. Specifically these are 50-72 eV, 66-100 eV, 95-111 eV, 107-147 eV, 141-187 eV, 181-283 eV, 260-454 eV, 440-574 eV, 558-600 eV, 596-776 eV, 752-932 eV, and 900-1300 eV. In addition, two more detailed ranges were selected for contaminant characterization for C- and O-K-edges, specifically 280-310 eV for C-K, and 520-562 eV for O-K.

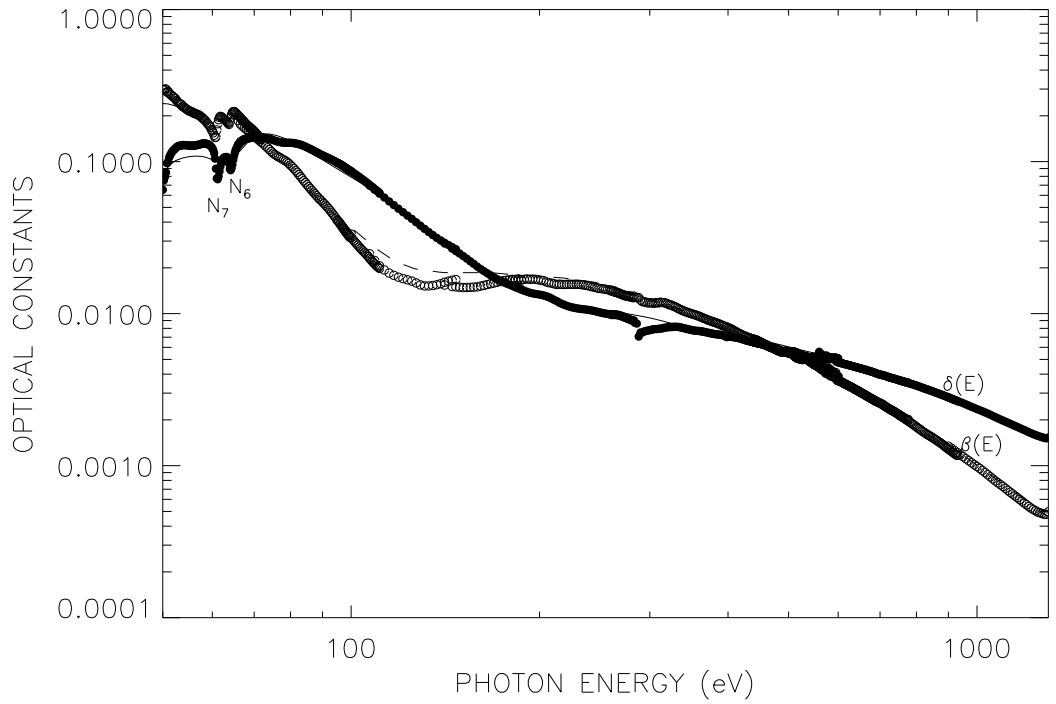

Figure 15: Preliminary optical constants derived from standard mirror 065 for the selected Beamline 6.3.2 range of 50-1300 eV. Optical constants from Ref 5 are included as curves, which are mostly overlain by the experimental data.

The eventual plan is to determine precisely the molecular nature of any overlayer(s) that may be present through independent measurement of the surface layer composition and thickness, and to include them in the energy-scan modeling. At this point we do not have a better model developed, and hence we can only follow through with the current one, and present the $\delta(E)$ and $\beta(E)$ results currently obtained as preliminary. Hence Fig. 15 for the fitted results for optical constants versus energy in the 50-1300 eV range, with the Ref. 5 constants included. The most striking features are the Ir N_7 and N_6 edges appearing prominently in the δ and β at 60.8 and 65.8 eV respectively. Clearly the tabulated constants do not show these features at all, and our results indicate an improvement to be made in the tabulations here.

In evidence are several spurious features, which may be due to the presence of contamination on the sample surface; however the beamline optics may also contain contaminants which were not successfully normalized from our data. First see the feature at 288 eV in the δ, which is clearly due to a C-related feature with a small chemical shift from the nominal 284 eV for C-K. Second, see the displacement of the $\beta(E)$ near the O-K and N-K regions, which overlap N-edge features of Ir. Some deconvolution of these effects will be necessary. Nevertheless, we have now a first cut at optical constants for the lowest energy range of Chandra, and an indication that the completion of the full 50-12000 eV calibration is at hand.

5. DISCUSSION AND SUMMARY

We have completed essentially all synchrotron reflectance measurements using the Brookhaven and ALS facilities as of November 1998, before the launch of Chandra, and within the funding and scheduling constraints of our program. Prior to launch, we provided optical constants from our standard mirror 065 covering the 940-12000 eV range, with acceptable overlap with the tabulated values at 940 eV. The analysis of the 940 – 12000 eV data indicates that each mirror has its own unique film layer depths and overlayer contaminant masking, but the optical constants of the iridium are quite consistent between the numerous witness flats.

We have now begun to analyze the results of our reflectance measurements at ALS Beamline 6.3.2. The results are still preliminary, and include measurements from only mirror 065. Notwithstanding, we have determined that the only strong Ir features are those due to N_7 and N_6 absorption edges. These features appear to be significant in the optical constants data, but their significance to Chandra effective area is lessened because of Chandra's grazing angle range, with all shells being of grazing angle less than 60 arc minutes. Individual reflecting efficiencies are only decreased by about 2% due to the N-edges at 51.87 arc minutes, the largest grazing angle (and largest mirror elements) included in the Chandra HRMA. The net effect on the effective area is at the level of 3-5% of the total area of Chandra at 60 eV. The narrowness of the features could affect line studies done on the Chandra LETG/HRC-S configuration to some degree, and so it would be considered important to have these edges characterized. The current tabulated data do not describe these features at all.

More relevantly for characterization of iridium as an X-ray material, our aim is to produce a definitive set of optical constants from our clearly large database of reflectance measurements. Our modeling of the overlayer, while adequate above 1000 eV, is in need of improvement in order to achieve the same level of certainty in optical constants below that energy. Therefore we need some independent determination of the overlayer, interface layers, coating depths (if possible), and other parameters we use in our analysis. This would lend more credence to our eventual optical constants for Ir. If successful, iridium could be one of the best-understood X-ray materials available. Considering the effort put into this calibration, that is certainly a reasonable goal for the community to anticipate from this work.

ACKNOWLEDGMENTS

The following individuals have participated in laboratory engineering, planning, measurements, or analysis for Chandra synchrotron reflectance calibrations, over the ten-year period of the planning and execution of this task, and we hereby express our gratitude for their participation: T. H. Burbine, A.M. Clark, J.P. Cobuzzi, J.J. Fitch, R. Francoeur, B. Harris, R.H. Ingram, J.Z. Juda, A.G. Roy, D.A. Schwartz, E.S. Sullivan, J.B. Sweeney, and P. Zhao. This list is not exhaustive, but includes the main participants. The authors are grateful for discussions and encouragement provided by the late L.P. Van Speybroeck, whom we remember fondly.

This work is supported by NASA (Contract Nos. NAS8-40224 and NAS8-39073) and by the US D.O.E. The Department of Energy supports the National Synchrotron Light Source (NSLS) at Brookhaven National Laboratory, and the Advanced Light Source (ALS) at Lawrence Berkeley Laboratory. The measurements over the 5-12 keV range were taken from NSLS Beamline X8A. Those covering 2010-6000 eV were taken from NSLS Beamline X8A. The 940-2030 eV measurements were taken using NSLS Beamline U3A. Those from 50-1300 eV were taken from ALS Beamline 6.3.2.

REFERENCES

[1] D.E. Graessle, R.L. Blake, A.J. Burek, S.E. Dyson, J.J. Fitch, D.A. Schwartz, and R. Soufli, "Modeling of synchrotron reflectance calibrations of AXAF iridium-coated witness mirrors over 2-12 keV," in *X-ray Optics, Instruments, and Missions*, ed. by R.B. Hoover and A.B.C. Walker II, *Proc. SPIE*, **3444**, pp. 140-159, 1998.

[2] D. L. Windt, "IMD-software for modeling the optical properties of multilayer films," Computers Phys. 12, 360-370, 1998. The IMD program is available at http://www.cletus.phys.columbia.edu/~windt/imd/.

[3] L. Nevot and P. Croce, "Caracterisation des surfaces par reflexion rasante de rayons X. Application a l'etude du polissage de quelques verres silicates," Rev. Phys. Appl. **15**, pp. 761-779, 1980.

[4] D.G. Stearns, *J. Appl. Phys.* **65** (2), pp. 491-502, 1989.

[5] B.L. Henke, E.M. Gullikson, and J.C. Davis, "X-ray interactions: photoabsorption, scattering, transmission, and reflection at E=50-30,000 eV, Z=1-92," in *Atomic Data and Nuclear Data Tables* **54**(2), p. 181, 1993. See also the Web page http://www-cxro.lbl.gov/optical_constants/.

[6] A.J. Burek, R.L. Blake, J.P. Cobuzzi, J.J. Fitch, R. Francoeur, D.E. Graessle, R.H. Ingram, E.S. Sullivan, and J.B. Sweeney, "The development of Beamline U3A for AXAF synchrotron reflectivity calibrations," in *X-ray Optics, Instruments, and Missions*, ed. by R.B. Hoover and A.B.C. Walker II, *Proc. SPIE*, **3444**, pp. 140-159, 1998.

[7] D.A. Schwartz, L.P. David, R.H. Donnelly, R.J. Edgar, T.J. Gaetz, D.E. Graessle, D. Jerius, M. Juda, E.M. Kellogg, B.R. McNamara, P.P. Plucinsky, L.P. Van Speybroeck, B.J. Wargelin, S. Wolk, P. Zhao, D. Dewey, H.L. Marshall, N.S. Schulz, R.F. Elsner, J.J. Kolodziejczak, S.L. O'Dell, D.A. Swartz, A.F. Tennant, M.C. Weisskopf, "Absolute effective area of the Chandra high-resolution mirror assembly (HRMA)," in *Proc. SPIE*, **4012**, pp. 28-40, 2000.

[8] J.H. Underwood, E.M. Gullikson, M. Koike, and P.J. Batson, "Beamline for metrology of X-ray/EUV optics at the Advanced Light Source," *Proc. SPIE*, **3113**, pp. 214-221, 1997.